Ultra-low-dose lung multidetector computed tomography in children - Approaching 0.2 millisievert

Tschauner, Sebastian ; Zellner, Michael ; Pistorius, Sarah ; Gnannt, Ralph ; Schraner, Thomas ; Kellenberger, Christian J

Abstract: PURPOSE To compare objective and subjective parameters in image quality and radiation dose of two MDCTs (helical 64 detector CT vs. axial 256 detector CT) in paediatric lung CT. METHODS Radiation dose and image quality were compared between non-enhanced lung CT from a helical 64-slice multidetector CT (MDCT 1) and a 256-slice scanner (MDCT 2) with axial wide-cone acquisition and using deep learning image reconstruction. In 23 size-matched paediatric studies (age 2-18 years) from each scanner, the radiation exposure, signal-to-noise ratio (SNR), contrast-to-noise ratio (CNR), image sharpness and delineation of small airways were assessed. Subjective image quality was rated by 6 paediatric radiologists. RESULTS While MDCT 2 provided higher SNR and CNR, subjective image quality was not significantly different between studies from both scanners. Radiation exposure was lower in studies from MDCT 2 (CTDIvol 0.26 ± 0.14 mGy, effective dose 0.23 ± 0.11 mSv) than from MDCT 1 (CTDIvol 0.96 ± 0.52 mGy, effective dose 1.13 ± 0.58 mSv), $p < 0.001$. Despite lower radiation dose for the scout images, the relative scout-scan-ratio increased from 2.64 ± 1.42 % in MDCT 1 to 6.60 ± 5.03 % in MDCT 2 ($p = 0.001$). CONCLUSIONS By using latest scanner technology effective radiation dose can be reduced to 0.1-0.3 mSv for lung CT in children without compromising image quality. Scout image dose increasingly accounts for substantial portions of the total scan dose and needs to be optimized. In children CT should be performed on state-of-the-art MDCT scanners with size-adapted exposure protocols and iterative reconstruction.

DOI: https://doi.org/10.1016/j.ejrad.2021.109699

European Journal of Radiology 139 (2021) 109699

Contents lists available at ScienceDirect

European Journal of Radiology

journal homepage: www.elsevier.com/locate/ejrad

Ultra-low-dose lung multidetector computed tomography in children – Approaching 0.2 millisievert

Sebastian Tschauner [a,b,1], Michael Zellner [a,*,1], Sarah Pistorius [a], Ralph Gnannt [a], Thomas Schraner [a], Christian J. Kellenberger [a]

[a] University Children's Hospital Zurich, Department of Imaging, Zurich, Switzerland
[b] Medical University of Graz, Department of Radiology, Division of Pediatric Radiology, Graz, Austria

ARTICLE INFO

Keywords:
Tomography
X-ray computed
Diagnostic imaging
Lung
Child
Radiation
Ionizing

ABSTRACT

Purpose: To compare objective and subjective parameters in image quality and radiation dose of two MDCTs (helical 64 detector CT vs. axial 256 detector CT) in paediatric lung CT.

Methods: Radiation dose and image quality were compared between non-enhanced lung CT from a helical 64-slice multidetector CT (MDCT 1) and a 256-slice scanner (MDCT 2) with axial wide-cone acquisition and using deep learning image reconstruction. In 23 size-matched paediatric studies (age 2–18 years) from each scanner, the radiation exposure, signal-to-noise ratio (SNR), contrast-to-noise ratio (CNR), image sharpness and delineation of small airways were assessed. Subjective image quality was rated by 6 paediatric radiologists.

Results: While MDCT 2 provided higher SNR and CNR, subjective image quality was not significantly different between studies from both scanners. Radiation exposure was lower in studies from MDCT 2 (CTDIvol 0.26 ± 0.14 mGy, effective dose 0.23 ± 0.11 mSv) than from MDCT 1 (CTDIvol 0.96 ± 0.52 mGy, effective dose 1.13 ± 0.58 mSv), $p < 0.001$. Despite lower radiation dose for the scout images, the relative scout-scan-ratio increased from 2.64 ± 1.42 % in MDCT 1 to 6.60 ± 5.03 % in MDCT 2 ($p = 0.001$).

Conclusions: By using latest scanner technology effective radiation dose can be reduced to 0.1−0.3 mSv for lung CT in children without compromising image quality. Scout image dose increasingly accounts for substantial portions of the total scan dose and needs to be optimized. In children CT should be performed on state-of-the-art MDCT scanners with size-adapted exposure protocols and iterative reconstruction.

1. Introduction

Paediatric radiologists dreamed of X-ray plain radiography equivalent doses in lung computed tomography (CT) for a long time. This desire has not yet been fulfilled due to simultaneous improvements of radiography detectors [1]. Multidetector row CT (MDCT) scanners allow lung CT doses of about 0.1 Millisievert (mSv) [2], commonly considered as the effective dose (ED) of an adult chest X-ray [3]. However, EDs of paediatric chest X-rays are typically a factor of ten or more lower today [4,5].

In order to raise community awareness, principles like "as low as reasonably achievable "(ALARA) [6] and campaigns such as Image Gently [7] lead toward a better understanding of radiation exposure. CT is still the largest cause for general and medical radiation exposure worldwide [8]. Studies about increased cancer risks in children who underwent CT [9,10] emphasize on the importance of paediatric CT radiation protection. The main dose reduction methods are X-ray beam shaping (e.g. tin filtering) [11], detector efficiency improvements [12],

Abbreviations: AAPM, The American Association of Physicists in Medicine; AP, anteroposterior; CT, computed tomography; CTDI, computed tomography dose index; DLIR, Deep Learning Image Reconstruction; DLP, dose length product; DRL, diagnostic reference level; Dw, water equivalent diameter; ED, effective dose; HU, Hounsfield unit; IQSC, image quality scoring criteria; kV(p), (peak) kilovoltage; LR, localizer radiograph; mA, milliampere; mAs, milliampere-second; MDCT, Multidetector Computed Tomography; mGy, milligray; ML, mediolateral; mSv, millisievert; ROI, region of interest; SD, standard deviation; SSDE, size specific dose index.

* Corresponding author at: Steinwiesstrasse 75, 8032 Zürich, Switzerland.
E-mail addresses: sebastian.tschauner@kispi.uzh.ch (S. Tschauner), michael.zellner@kispi.uzh.ch (M. Zellner), sarah.pistorius@kispi.uzh.ch (S. Pistorius), ralph.gnannt@kispi.uzh.ch (R. Gnannt), thomas.schraner@kispi.uzh.ch (T. Schraner), christian.kellenberger@kispi.uzh.ch (C.J. Kellenberger).
[1] Contributed equally.

https://doi.org/10.1016/j.ejrad.2021.109699
Received 19 December 2020; Received in revised form 29 March 2021; Accepted 5 April 2021
Available online 22 April 2021

automated tube voltage selection and tube current selection [13], and iterative reconstruction algorithms including artificial intelligence methods [14,15].

MDCT devices allow for helical and axial scanning. In wide detectors of up to 16 cm, axial scanning is possible without table movement and is therefore beneficial in paediatric imaging [16].

The aim of the study was to compare objective and subjective parameters in image quality and radiation dose of two different MDCTs (helical 64 detector CT vs. axial 256 detector CT) in paediatric lung CT examinations.

2. Material and methods

The local Department of Diagnostic Imaging substituted its single MDCT scanner in December 2019. A Revolution CT (GE Healthcare, Chicago, Illinois, United States of America) 256 row multidetector device replaced the Brilliance 64 CT (Philips Healthcare, Amsterdam, Netherlands) 64 row multidetector machine. "MDCT 1" denotes the old, "MDCT 2" the new device throughout the manuscript. Table 1 lists selected scanner characteristics. MDCT 2 images were reconstructed with enabled deep-learning iterative reconstruction (DLIR), which uses machine learning techniques to reduce image noise and improve image quality [17]. After the replacement, chest studies were initially performed in helical mode with scan parameters similar to the previous machine. Due to overly satisfying image quality, we gradually lowered exposure settings over the following weeks. The axial scan mode (without table increment) supplanted helical scanning with increasing frequency. 47 consecutive patients underwent 52 axial low-dose CTs of the chest between December 2019 and May 2020 on MDCT 2. All MDCT 2 studies were acquired with fixed exposure parameters, specifically without automated tube voltage selection or tube current modulation. We excluded examinations with non-lung-specific clinical questions or exposure protocol. We matched the remaining studies to MDCT 1 examinations, performed between July 2017 and November 2019. Matching criteria included identical gender, effective chest diameter ±10 mm, age at examinations within 1 year. Moreover, all studies needed to be in inspiration (breath hold inspiration or free-breathing, not in expiration), arms positioned above the head, and without intravenous contrast agent. Thin collimation slices (0.625 mm) needed to be archived in the PACS, which did not contain proper matching studies in 4 cases.

Finally, we included 23 study pairs. Fig. 1 depicts the described examination selection procedure. Included samples mean patient age was 10.8 ± 4.9 (range 1.7–17.3 years) years in MDCT 1 and 11.1 ± 5.0 (range 2.0–18.2 years) years in MDCT 2, with 13 female and 10 male examination pairs. AP chest diameters averaged 17.3 ± 3.3 (range 11.9–23.3 cm) in MDCT 1 and 17.8 ± 3.4 (range 12.0–23.5 cm) in MDCT 2. Mediolateral (ML) chest diameters were 26.9 ± 4.9 (range 18.3–37.1 cm) in MDCT 1 and 26.9 ± 5.5 (range 18.5–37.3 cm) in MDCT 2 on average. We calculated effective chest diameters based on the AAPM report 204 [18] as $\langle \sqrt[2]{[anteroposterior\ (AP)\ *\ mediolateral\ (ML) chest\ diameter]} \rangle$, rounded to full centimeters. On average, effective chest diameter was 22 ± 4 cm (range 16–29 cm) in MDCT 1, and 22 ± 4 cm (range 15–29 cm) in MDCT 2. Water equivalent diameter (D_w) was derived from AAPM publication 220 [19] by summing AP and ML chest diameters. Mean D_w was 23 ± 4 cm (range 16–31 cm) in MDCT 1, and 23 ± 4 cm (range 16–30 cm) in MDCT 2. We noted no relevant difference between effective and water equivalent diameters.

2.1. DICOM anonymization

S.T. anonymized and exported all studies from Workstation 21.2 (Sectra AB, Linköping, Sweden) to a local storage device. Randomly assigned ID numbers served as examination mixing procedure. We synchronized a standard lung window (centre -500 Hounsfield units (HU), window width 1500 HU) across all lung kernel series. Each observer loaded the batch of anonymized examinations in synedra View 18 (synedra information technologies GmbH, Innsbruck, Austria) to rate them on calibrated 10-bit colour monitors Radiforce RX340 (EIZO Corporation, Hakusan, Ishikawa, Japan) in darkened reading rooms.

2.2. Objective image quality measurements

The first author manually placed circular regions of interest (ROI) in thin axial lung window slices (0.625 mm) to retrieve the HU mean and standard deviation, the latter representing image noise. The minimum allowed ROI area was 5000 pixels. The average of three repeated measurements in

- the dome of the right liver lobe,
- the whole heart at the level of the left ventricle,
- and the air space anteriorly to the mid chest

Table 1
Acquisition and image reconstruction settings used in the study MDCT devices.

		MDCT 1 (Philips Brilliance)	MDCT 2 (GE Revolution)	Significant differences (p)
Scanner properties	Installed in, *year*	2003	2019	–
	Detector rows, *N*	64	256	–
	Slice collimation, *mm*	0.625	0.625	–
	Detector width, *mm*	40	160	–
Localizer radiograph	kV	80	70	–
	mA	20	10	–
Image acquisition	Used scan mode	helical	axial	–
	Rotation / exposure time, *sec*	0.625	0.280	$p < 0.001$
	Field of view, *mm* (mean ± SD)	252 ± 43	276 ± 47	$p = 0.070$
	kVp (mean ± SD)	87.8 ± 10.0	110.4 ± 11.9	$p < 0.001$
	mA (mean ± SD)	52.9 ± 13.2	14.1 ± 4.9	$p < 0.001$
	mAs (mean ± SD)	33.0 ± 8.2	3.9 ± 1.4	$p < 0.001$
Image reconstruction	Planes	axial, coronal, sagittal	axial, coronal, sagittal	–
	Kernel	Lung	Standard lung	–
	Iterative reconstruction	iDose[4]	DLIR medium	–
	Pixel matrix	512 × 512	512 × 512	–
	Reconstructed slice thickness, *mm*	0.625 / 1.0 (MPR average)	0.625 / 1.0 (MPR average)	–
	Pixel spacing, *mm* (mean ± SD)	0.49 ± 0.08	0.54 ± 0.09	$p = 0.070$
Radiation doses	$CTDI_{vol}$ [32 cm phantom], *mGy* (mean ± SD)	0.96 ± 0.52	0.26 ± 0.14	$p < 0.001$
	SSDE, *mGy* (mean ± SD)	1.52 ± 0.69	0.41 ± 0.19	$p < 0.001$
	DLP scout, *mGy*cm* (mean ± SD)	0.60 ± 0.22	0.29 ± 0.11	$p < 0.001$
	DLP scan, *mGy*cm* (mean ± SD)	32.37 ± 21.80	6.65 ± 4.44	$p < 0.001$
	Scout-scan-ratio, *%*	2.64 ± 1.42	6.60 ± 5.03	$p = 0.001$
	ED, *mSv* (mean ± SD)	1.13 ± 0.58	0.23 ± 0.11	$p < 0.001$

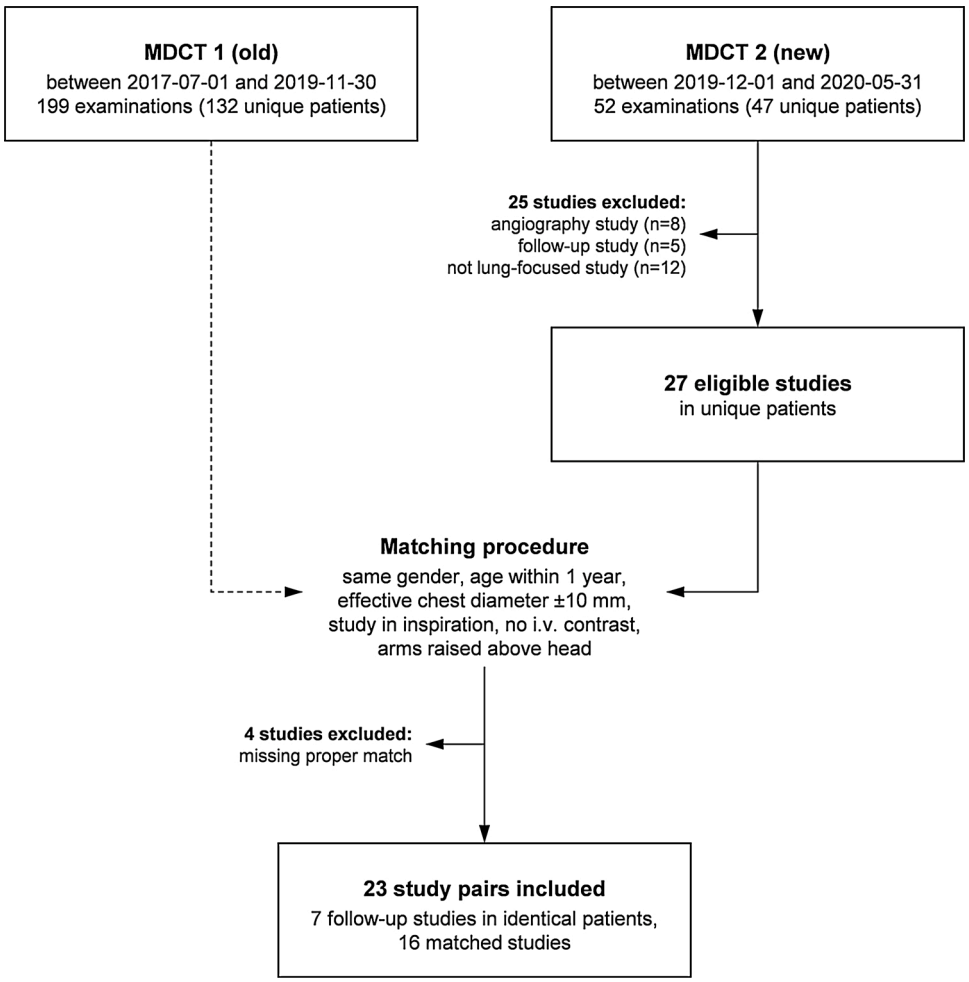

Fig. 1. Flowchart depicting the study selection procedure. i.v. = intravenous.

acted as basic objective image quality parameters. Based on these parameters, we calculated signal-to noise $\langle = SNR = \frac{MEAN\ tissue\ (HU)}{SD\ tissue\ (HU)} \rangle$ and contrast-to-noise $\langle = CNR = \frac{MEAN[MEAN(liver, heart)]\ (HU) - MEAN\ air\ (HU)}{SD\ air\ (HU)} \rangle$ ratios.

Moreover, we followed the tracheobronchial tree into the lower lobes, noting the generations of the smallest perceptible bronchi (trachea = generation 0) as a surrogate parameter for image sharpness.

2.3. Subjective image quality ratings

S.T. (8-year experience in lung CT) and M.Z. (5-year experience in lung CT) consensually scored subjective image quality parameters (focusing on lung tissue) and artifacts (Fig. 2) on a five-point rating scale (0 = very blurred, 1 = blurred, 2 = neither blurred nor sharp, 3 = sharp, 4 = very sharp). Artifacts were also scored on a five-point rating scale (0 = no artifacts, 1 = minimum artifacts, 2 = minor artifacts, 3 = moderate artifacts, 4 = major artifacts). Additionally, we used an IQSC (Image Quality Scoring Criteria) -based score with "interstitial lung pathology" indication to establish general subjective image quality of each study [20]:

1 Unacceptable quality (images do not allow diagnostic interpretation)
2 Limited quality (images are adequate only for limited clinical interpretation due to high noise)
3 Adequate quality (images are just adequate for diagnostic interpretation)
4 Higher than needed quality (images are much better than needed for interpretation: images with little or no noise) [20]

Six observers independently scored the IQSC (C.K. = Rater 1, M.Z. = Rater 2, R.G. = Rater 3, S.P. = Rater 4, S.T. = Rater 5, and T.S. = Rater 6), with chest CT experiences of 27, 5, 11, 7, 8, 23 years, cumulating to 81 years.

2.4. Dose estimates

We collected the computed tomography dose indices (=$CTDI_{vol}$, 32 cm phantom, mGy) and the dose length products $\langle = DLP = CTDIvol * scan\ lenth\ in\ cm\ (mGy * cm) \rangle$ for scouts and scans from the DICOM dose reports. The effective diameters together with the size-dependent correction factors, derived from the publications by the AAPM [18,19] and by Romanyukha et al. [21], served as calculation basis for size specific dose estimates (=SSDE, *mGy*) and effective doses (=ED, *mSv*), the latter calculated as DLP multiplied with the diameter-specific conversion factor [21].

2.5. Statistical analysis

We analysed the collected data in SPSS Statistics Version 21 (IBM Corp., Armonk, NY, USA) by computing descriptive statistics, linear correlation analysis, as well as *t*-test mean value comparisons in cases of ascertained, and nonparametric Mann–Whitney U tests in missing normal distributions. For sub-group analyses, we split study pairs by age groups from 0 to 5 years (n = 4, age group 1), 6–10 years (n = 6, group

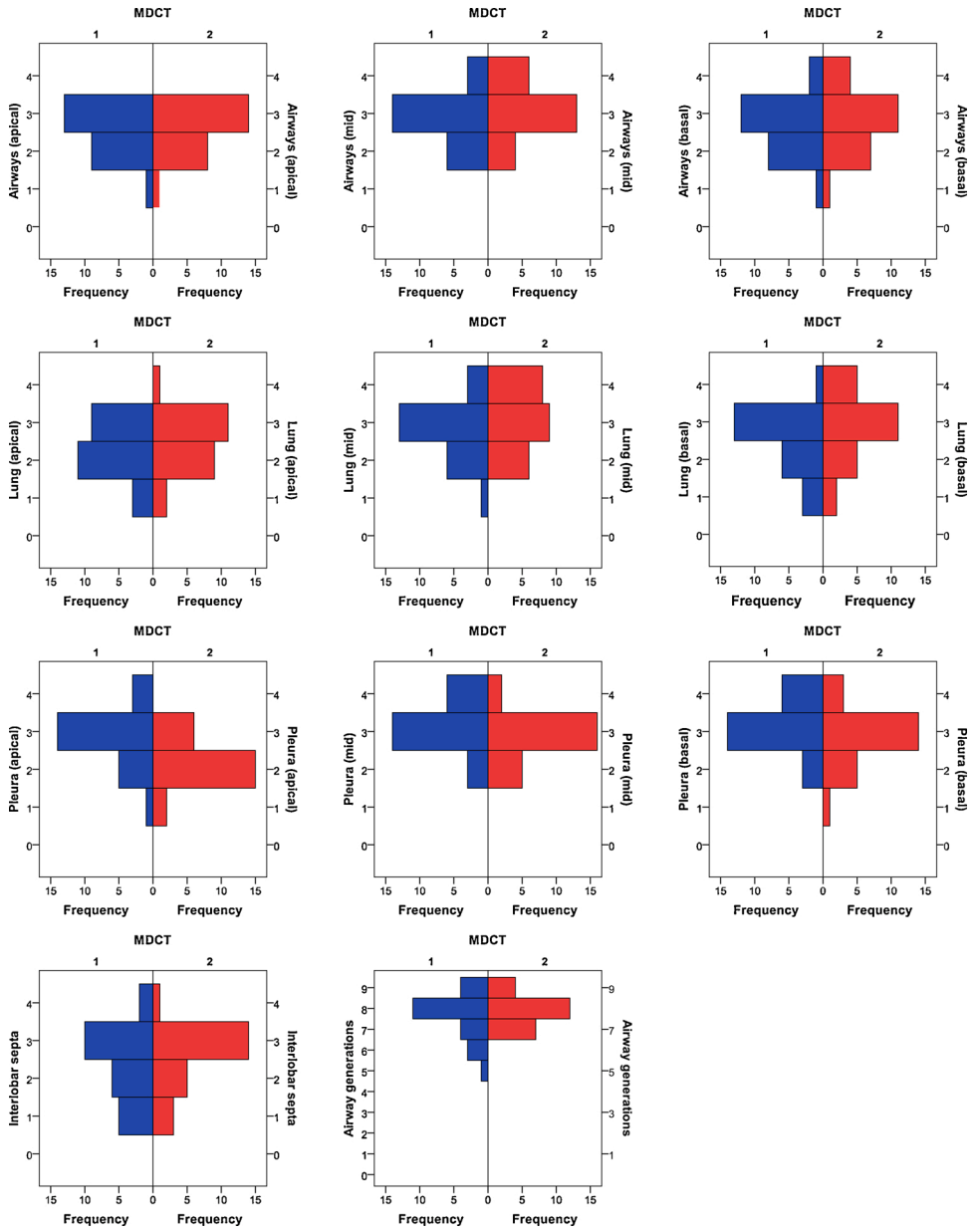

Fig. 2. MDCT 1 in blue bars, MDCT 2 in red bars a) Frequency histograms of subjective image quality ratings and b) Frequency histograms of image artifacts.

2), 11–15 years (n = 7, group 3), and 16–18 years (n = 6, group 4). Throughout this manuscript, the significance level was set to p = 0.050. One-sided non-inferiority t-tests were calculated using Statgraphics Centurion 19 (Statgraphics Technologies Inc., The Plains, VA, USA), to assess our hypothesis that image quality was not inferior in MDCT 2. Prior to the statistical analyses, the authors consensually agreed on the non-inferiority cut-off of 0.5 points as the clinically relevant margin. P-values below the significance level demonstrated the non-inferiority of specific MDCT 2 parameters. Intraclass correlation coefficients (ICC) served as measures of inter-observer reliability in terms of ICC(3,k) two-way mixed, average measures. ICC values below 0.5 refer to poor, 0.5 to 0.75 moderate, 0.75 to 0.9 good, and higher than 0.9 to an excellent reliability [22].

2.6. Ethics committee

The local Ethics committee of the Canton of Zurich, Switzerland, approved the study (No. 2020-01644). We obtained written informed patient or legal representative consent in all included cases.

3. Results

Mean background noise was 83.0 ± 20.4 HU in MDCT 1 and 46.4 ± 8.6 HU in MDCT 2 (*t*-test $p < 0.001$). CNR was 13.2 ± 3.8 HU in MDCT 1 and 23.2 ± 3.5 HU in MDCT 2 (*t*-test $p < 0.001$). SNR liver was 0.25 ± 0.07 in MDCT 1 and 0.85 ± 0.21 HU in MDCT 2 (*t*-test $p < 0.001$). SNR heart was 0.26 ± 0.06 in MDCT 1 and 0.51 ± 0.12 HU in MDCT 2 (*t*-test $p < 0.001$). We noted a significant negative linear correlation of image noise with both SSDE and ED in MDCT 1 ($p < 0.001$), whereas noise was relatively stable across different dose levels in MDCT 2 due to DLIR. SSDE und ED increased with age, predominantly in MDCT 1 (Supplementary Fig. 1). MDCT 2 showed significant dose reductions over MDCT 1 in terms of decreased $CTDI_{vol}$, DLP, SSDE, and ED values (*t*-test all $p < 0.001$). Only the scout-scan-ratio increased substantially ($p = 0.001$). Table 1 lists the respective radiation dose parameters.

Median kVp settings were 80, 80, 100, 100 kVp for age groups 1–4 in MDCT 1, and 100, 100, 120, 120 in MDCT 2. Median effective tube current settings were 20, 30, 40, 40 mAs in age groups 1–4 in MDCT 1, and 2.8, 3.5, 5.6, and 4.2 mAs in MDCT 2. The resulting mean effective

doses were 0.54 ± 0.04, 0.75 ± 0.10, 1.36 ± 0.65, 1.63 ± 0.32 mSv for age groups 1–4 in MDCT 1, and 0.12 ± 0.01, 0.16 ± 0.04, 0.30 ± 0.08, 0.29 ± 0.14 mSv in MDCT 2. Supplementary Table 1 shows IQSC ratings for the different examination pairs and raters split into the mentioned age groups.

Both scanners received a median IQSC of 3, ranging from 2 to 4 in MDCT 1, and 1–4 in MDCT 2 (non-inferiority *t*-test $p < 0.001$). The raters regarded 67 % of the studies conducted on MDCT 1 as adequate, while 8% were of limited and 25 % of higher than needed quality. In MDCT 2, 61 % of the studies were adequate, 14 % limited, and 25 % too high. One MDCT 2 examination received ratings of 1 (unacceptable image quality) by two of the observers. IQSC interrater agreement in terms of ICC scores were 0.780 (95 % CI 0.604 to 0.895) in MDCT 1 and 0.889 (95 % CI 0.800 to 0.947) in MDCT 2, which is considered a good consensus. Table 2 displays all IQSC ratings. The two most experienced paediatric radiologists (raters 1 and 6) considered more studies with a higher than necessary dose (*U* test $p < 0.001$), rater 1 primarily in MDCT 1, rater 6 in MDCT 2 (Table 2). Specific subjective image quality parameters were not statistically significantly inferior in MDCT 2, apart from pleural sharpness in all three lung fields (non-inferiority *t*-test apical $p = 0.784$, mid $p = 0.087$, and basal $p = 0.165$). We noted no significant differences between the sharpness of airways and lung tissue, generations of visible bronchi, and the depiction of the interlobar septa. Fig. 3 and Table 3 summarize the respective findings.

MDCT 2 scans demonstrated less cardiac pulsation artifacts (median 1 range 3 vs. median 2 range 3 in MDCT 1, *U* test $p < 0.001$), and more ring artifacts (median 0 range 1 vs. median 0 range 0 in MDCT 1, *U* test $p = 0.019$). Based on the axial scanning technique, only MDCT 2 examinations exhibited stitching artifacts (median 0 range 3 vs. median 0 range 0 in MDCT 1, *U* test $p = 0.005$). We detected no significant scanner differences regarding beam hardening artifacts (median 0 range 2 in both MDCTs, *U* test $p = 0.483$), and motion artifacts (median 0 range 1 in MDCT 1, and median 0 range 0 in MDCT 2, *U* test $p = 0.153$).

4. Discussion

In this study, we compared image quality and radiation doses in ultra-low-exposure paediatric lung imaging on two different MDCT, a helical 64-slice multidetector CT (MDCT 1) and a 256-slice scanner (MDCT 2). Imaging on MDCT 2 led to a dose reduction of about 80 % with preserved acceptable image quality when compared to MDCT 1. Despite increased CNR and SNR values in MDCT 2, caused by DLIR noise reduction, subjective IQSC ratings were at comparable levels.

The AAPM "Pediatric Chest Routine" document recommends chest CT exposure protocols for different CT scanners [23]. Suggested MDCT 2 settings exceed the radiation doses used in the current study. The AAPM authors state $CTDI_{vol}$ ranges of 1.9–2.5 mGy (32 cm phantom) in lateral chest diameters from 7 to 11 cm (small child), up to 5.2–8.8 from 29 to 33 cm (adolescent). Our patients received $CTDI_{vol}$ values of 0.11 to 0.58 on the MDCT 2 with sufficient image quality for lung reporting. It should be mentioned that doses for a full chest CT including mediastinum and possible contrast administration might require doses up to the AAPM recommendations. In this regard, MDCT 2 doses reported in the current study were substantially lower than diagnostic reference levels (DRLs) typically found in the literature [24,25]. As reported by Jarvinen et al., different scan indications and patient age are important factors to consider when assessing DRLs [26].

Subjective image quality interrater agreement was good. IQSC ratings were slightly better in MDCT 2. Interestingly, the most experienced paediatric radiologists rated more examinations as unnecessarily overexposed in both scanners. This underlines the difficulty to judge the proper radiation dose for paediatric lung imaging. Choosing the right exposure and reconstruction parameters will very likely stay a matter of debate and personal preference. We decided not to include advanced quantitative image quality metrics like "task based transfer function" [17] or "noise power spectrum" [27], because the added value in non-phantom studies is questionable. However, we want to emphasize again on the importance of subjective image quality assessments, and the limited comparability of objective and semi-objective quality metrics based on noise properties.

Predominantly in MDCT 2 and mainly in the apical lung portions, photon starvation caused image quality impairments in terms of pleural and lung blurring (Figs. 4 and 5). Moreover, extensive lung consolidation can impair image quality. Therefore, ultra-low-dose protocols are not adequate for soft tissue (mediastinum, liver etc.) assessment and display these areas in non-diagnostic quality.

We came across a hurdle in further reducing radiation exposure in MDCT 2 caused by a lower generator limit of 10 mA. Lung-focused CT primarily is a high-contrast scenario with substantial density differences between air and typically soft tissue-like pathologic processes. Therefore, it could be beneficial for lung-focused CT scanning to use higher kV settings with low mA to avoid image quality impairments through scatter and photon starvation. Other manufacturers successfully took similar approaches in a more aggressive way by reducing radiation doses through X-ray beam hardening, for example tin (Sn) filtering, also called spectral shaping or spectral filtering [2,11]. Our MDCTs did not provide spectral filtering.

Axial scanning in MDCT 2 resulted in specific stitching artifacts (compare Fig. 5) through appending axial volumes in scan ranges more than 16 cm [28]. These scan volume alignment errors due to patient movement, breathing, and pulsation might be of relevance detecting lung nodules. The artifact could clip pathologies in the stitching zones. Helical scanning effectively avoids stitching artifacts. While relevant in

Table 2
Summarized IQSC scores of all six raters in both MDCT devices. Color-coded scores between 1 (yellow) and 4 (green). (For interpretation of the references to colour in this table legend, the reader is referred to the web version of this article).

Examination pair		1	2	3	4	5	6	7	8	9	10	11	12	13	14	15	16	17	18	19	20	21	22	23
MDCT 1	Rater 1	3	3	4	4	3	4	3	4	3	3	3	3	3	3	3	3	3	3	3	4	4	3	3
	Rater 2	3	4	3	4	3	4	3	4	3	2	4	3	3	4	3	3	3	3	4	4	4	3	3
	Rater 3	3	3	4	4	3	3	3	3	3	2	4	3	3	4	3	3	3	3	3	3	3	3	3
	Rater 4	2	3	3	3	3	3	3	3	3	2	3	2	3	3	3	3	3	3	2	3	3	3	3
	Rater 5	2	3	4	3	3	3	3	3	2	2	3	3	4	3	3	3	3	3	3	2	4	4	3
	Rater 6	3	3	4	4	4	4	4	4	3	2	4	3	3	4	4	4	3	3	3	4	4	3	3
MDCT 2	Rater 1	3	3	4	3	4	2	4	4	4	3	3	4	3	4	4	3	4	4	4	3	3	3	3
	Rater 2	3	3	3	3	4	2	4	3	4	2	3	3	3	3	4	3	4	3	3	3	4	3	3
	Rater 3	2	2	4	4	4	1	4	3	4	3	3	3	3	3	4	4	4	3	4	2	4	2	3
	Rater 4	2	3	3	3	3	2	3	3	3	3	3	3	3	3	3	3	3	3	3	2	3	3	3
	Rater 5	2	3	3	3	3	1	4	3	3	3	3	3	3	3	4	3	3	3	3	2	3	2	2
	Rater 6	3	3	3	4	4	2	4	3	4	3	3	3	3	3	3	4	3	3	3	2	4	2	3

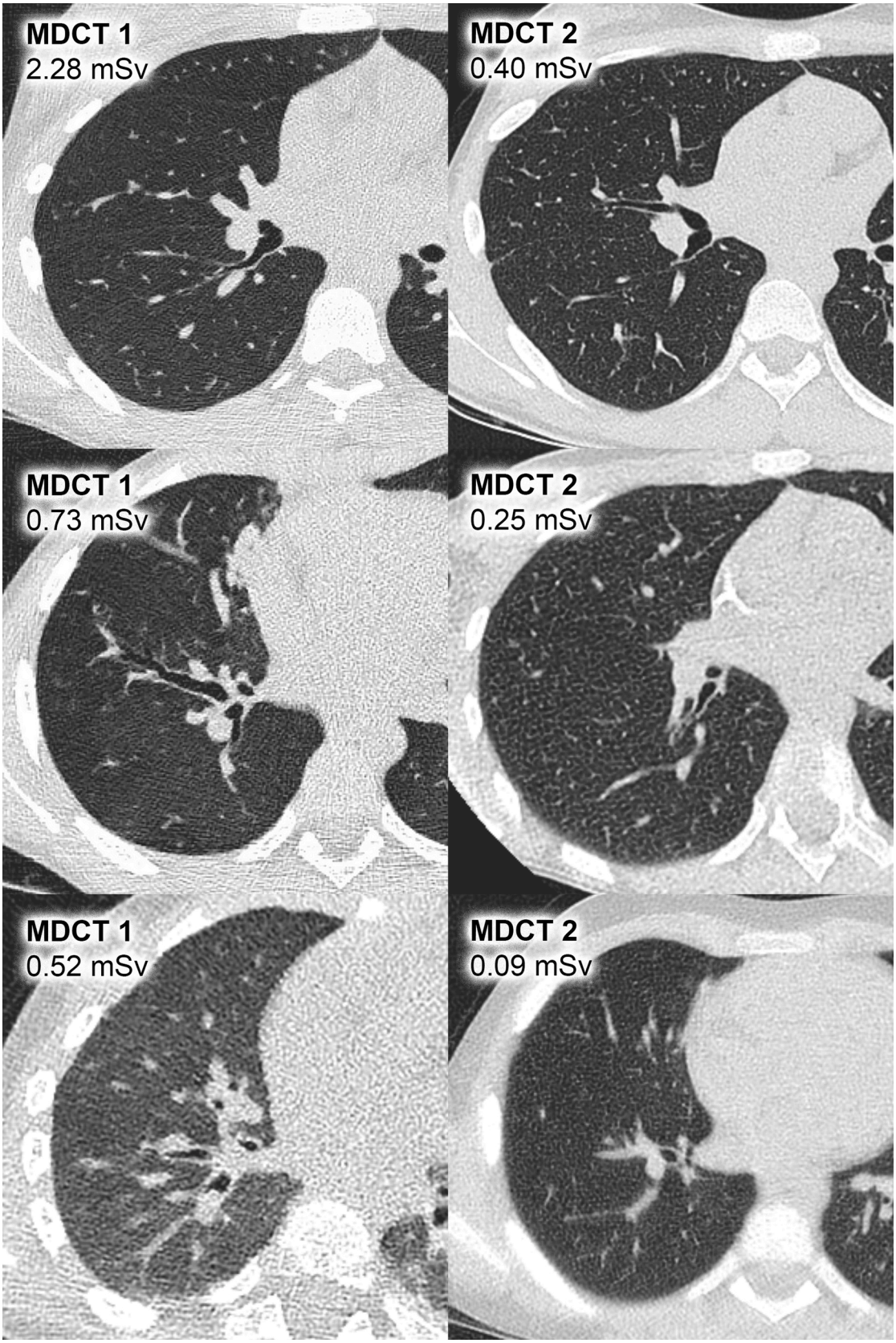

Fig. 3. Examples of examinations rated with too-high dose (IQSC grade 4) in the first row, adequate image quality (IQSC grade 3) in the second row, and too low dose (IQSC grade 2) in the third row.

Table 3
Subjective image quality assessment (mean and SD, median, range, minimum, maximum) including significant differences in U tests, marked with an asterisk. The ‡ marks parameters where non-inferiority was not statistically significant, meaning that MDCT 2 demonstrated inferior image quality in these parameters.

		Airways				Lung			Pleura			
		apical	mid	basal	gener-ations	apical	mid	basal	apical	mid	basal	Inter-lobar septa
	N	23	23	23	23	23	23	23	23	23	23	23
	Mean	2.52	2.87	2.65	7.61	2.26	2.78	2.52	2.83	3.13	3.13	2.39
	STD	0.59	0.63	0.71	1.08	0.69	0.74	0.79	0.72	0.63	0.63	0.94
MDCT 1	**Median**	3	3	3	8	2	3	3	3	3	3	3
	Range	2	2	3	4	2	3	3	3	2	2	3
	Minimum	1	2	1	5	1	1	1	1	2	2	1
	Maximum	3	4	4	9	3	4	4	4	4	4	4
	N	23	23	23	23	23	23	23	23	23	23	23
	Mean	2.57	3.09	2.78	7.87	2.48	3.09	2.83	2.17	2.87	2.83	2.57
	STD	0.59	0.67	0.80	0.69	0.73	0.79	0.89	0.58	0.55	0.72	0.79
MDCT 2	**Median**	3	3	3	8	3	3	3	2	3	3	3
	Range	2	2	3	2	3	2	3	2	2	3	3
	Minimum	1	2	1	7	1	2	1	1	2	1	1
	Maximum	3	4	4	9	4	4	4	3	4	4	4
Difference (p)		0.780	0.258	0.565	0.577	0.318	0.209	0.217	**0.001***	0.138	0.151	0.487
Non inferiority (p)		0.002	<0.001	0.004	0.003	0.001	<0.001	0.001	**0.784‡**	**0.087‡**	**0.165‡**	0.021

oncologic imaging, we think the artifact is of minor influence in most other pulmonary CT indications.

The CT localizer radiograph (=LR, also known as scout, survey scan, pilot scan, topogram, etc.) to the scan ratio raised from 2.6 % in the old to 6.6 % in the new scanner. The maximum scout-scan-ratio was 19 % in a 4-year-old. We noted this significant relative increase despite an absolute scout dose halving from 0.6 to 0.3 mGy*cm, because actual scan doses decreased even more. MDCT 1 LR were performed with 80 kVp and 20 mA, and with 70 kVp and 10 mA in MDCT 2. Authors previously published the necessity of optimizing the LR especially for paediatric patients [29,30]. While we agree that optimizations are important, some proposed methods seem to be unsuitable, as they might exceed the dose of a whole scan [31].

Limitations of our study include a small sample size and the fact that only a part of the examinations could be performed in identical patients. To compensate for this issue, we applied a rigorous matching strategy that only allowed a small variance in age, body dimensions, and scan indications. Another limitation is inherent to the different types and generations of CT scanners. MDCT 2 employs techniques like deep-learning based iterative image reconstruction algorithms, faster rotation times as well as a larger and more-sensitive detector. However, basic image reconstruction parameters like reconstructed slice thickness were identical across the machines, enabling a general comparability. We also want to mention that average peak kilovoltage (kVp) was lower in MDCT 1. A kVp difference infers with radiation exposure in terms of lower-energy X-ray beams suffer more tissue absorption. Higher kVp settings in the old device could have led to lower patient doses and might have mitigated the substantial dose discrepancies between the MDCTs.

5. Conclusions

Sufficient-quality paediatric lung CT can be achieved at effective radiation doses of 0.1 to 0.3 mSv on contemporary MDCT equipment. Localizer radiograph doses increasingly account for substantial portions of a total scan's doses and should be optimized. Rapid progress in scanner technique emphasizes the necessity to scan paediatric patients on contemporary equipment.

Funding

The authors state that this work has not received any funding.

Guarantor

The scientific guarantor of this publication is Christian J. Kellenberger.

Statistics and biometry

One of the authors has significant statistical expertise.

Methodology

Methodology:

- retrospective
- performed at one institution

Author contributions statement

Sebastian Tschauner, Michael Zellner and Christian J. Kellenberger contributed to the study concept. Data acquisition was performed by Sebastian Tschauner, Michael Zellner, Sarah Pistorius, Ralph Gnannt, Thomas Schraner and Christian J. Kellenberger. Data analyses and visualization were conducted by Sebastian Tschauner and Michael Zellner. Michael Zellner prepared the manuscript draft. Sebastian Tschauner, Sarah Pistorius, Ralph Gnannt, Thomas Schraner and Christian J. Kellenberger contributed to reviewing and editing of the manuscript. Christian J. Kellenberger supervised the project.

Ethical approval and informed consent

Approval of the study protocol (No. 2020-01644) was obtained from the Ethics committee of the Canton of Zurich, Switzerland, requiring informed consent of patients and/or legal representatives. All study-related methods were conducted in accordance with the Declaration of Helsinki and all relevant guidelines and regulations.

Data availability

A complete anonymized dataset of all measurements and the corresponding image data is stored at the author's institution.

Declaration of Competing Interest

The authors of this manuscript declare no relationships with any companies, whose products or services may be related to the subject matter of the article.

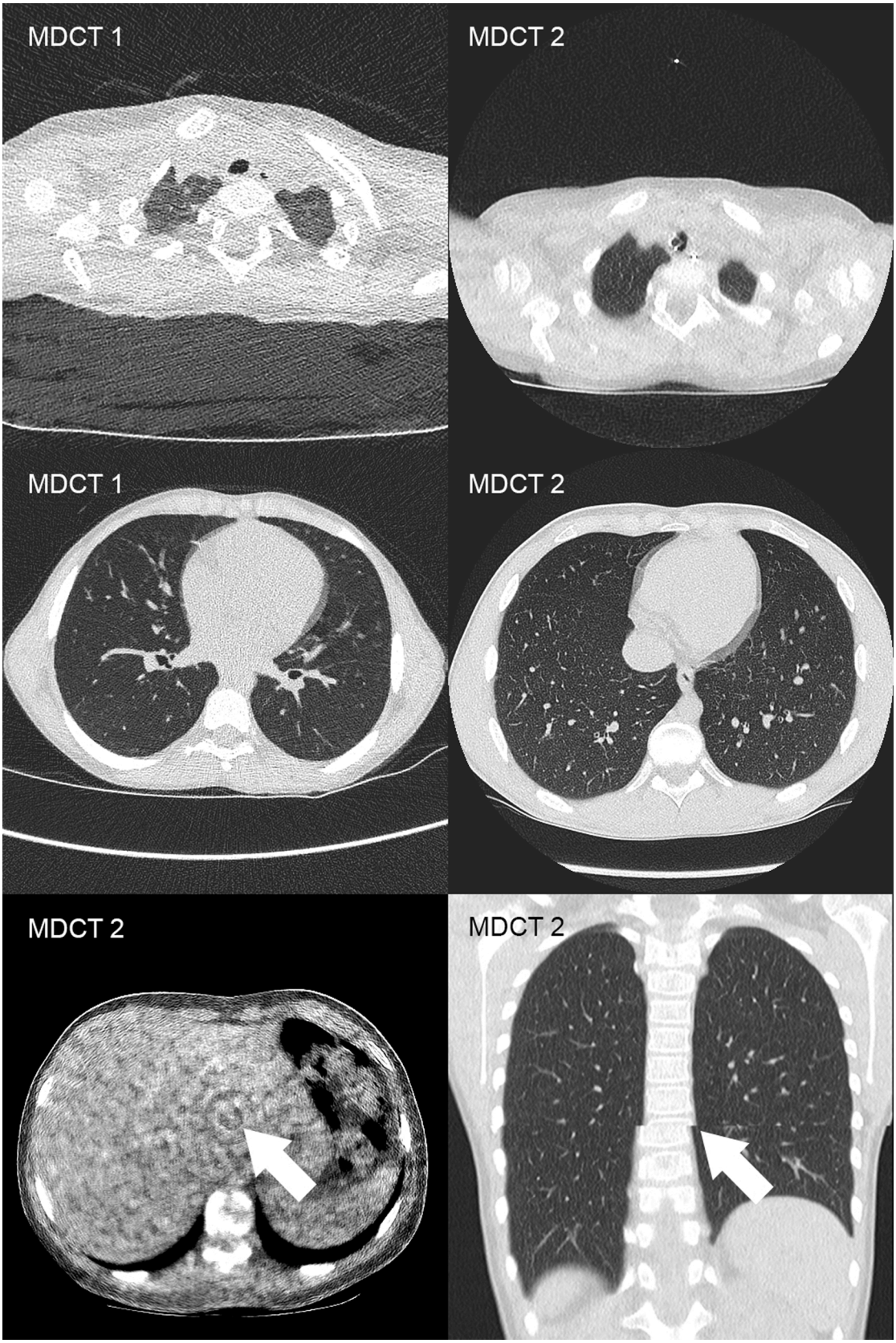

Fig. 4. Examples of image artifacts. Blurring of the pleura due to photon starvation in the apical lung areas in the first row. Cardiac pulsation artifacts in the second row. A ring artifact in the third row on the left, a stitching artifact of the 2 axial volume stacks on the right.

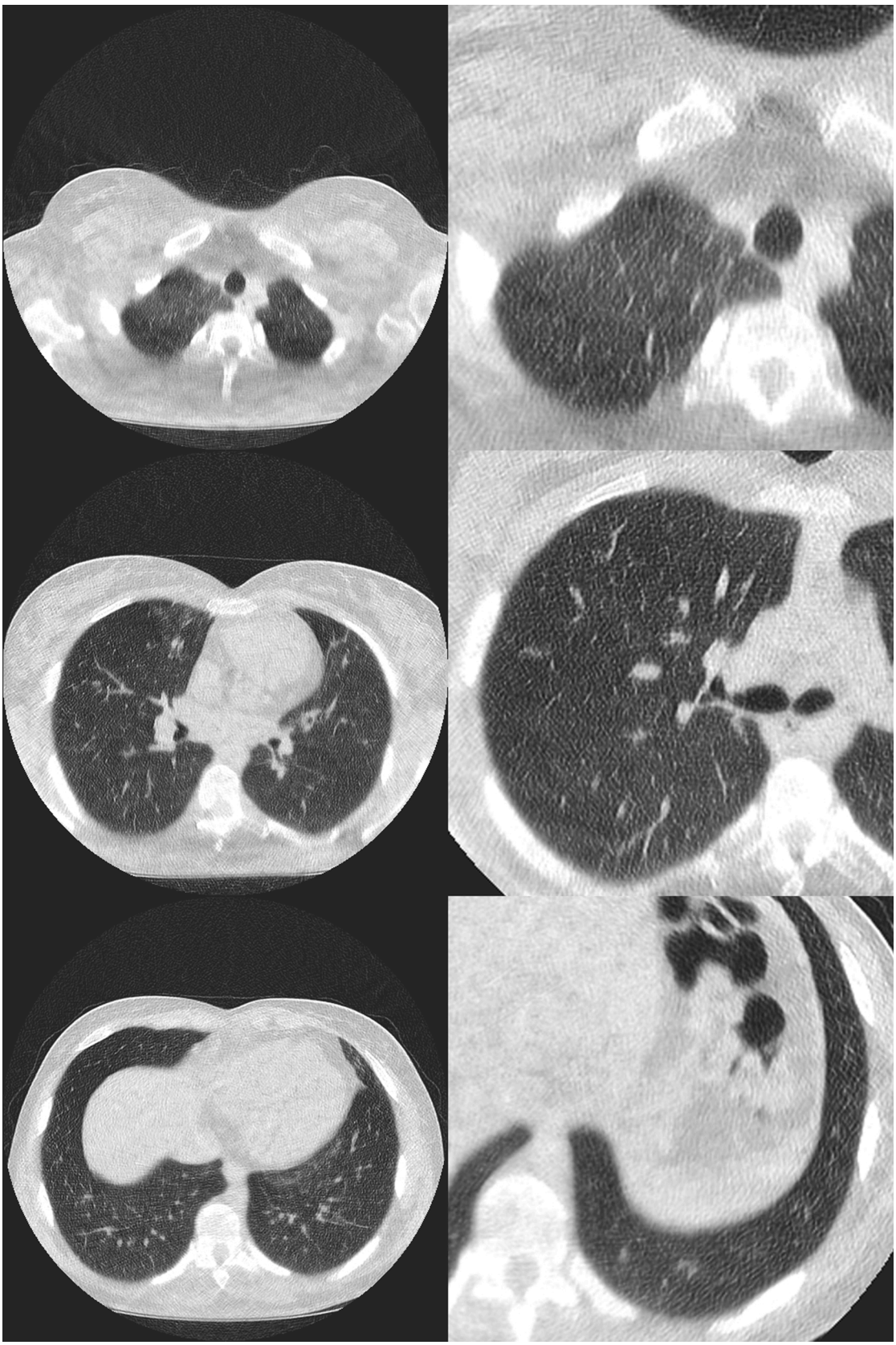

Fig. 5. Exemplary slices of a lung CT in a 17-year-old patient, considered unacceptable to limited quality, conducted on MDCT 2 with 100 kVp, 10 mA, 2.8 mAs, 0.9 mSv. Left row shows full FOV, right magnified sections (slices not corresponding). Note the partially substantial loss of details due to photon starvation, especially apical (first row).

Acknowledgements

None.

Appendix A. Supplementary data

Supplementary material related to this article can be found, in the online version, at doi:https://doi.org/10.1016/j.ejrad.2021.109699.

References

[1] E. Samei, N.T. Ranger, A. MacKenzie, I.D. Honey, J.T. Dobbins 3rd, C.E. Ravin, Effective DQE (eDQE) and speed of digital radiographic systems: an experimental methodology, Med. Phys. 36 (8) (2009) 3806–3817.
[2] S. Gordic, F. Morsbach, B. Schmidt, T. Allmendinger, T. Flohr, D. Husarik, S. Baumueller, R. Raupach, P. Stolzmann, S. Leschka, T. Frauenfelder, H. Alkadhi, Ultralow-dose chest computed tomography for pulmonary nodule detection: first performance evaluation of single energy scanning with spectral shaping, Invest. Radiol. 49 (7) (2014) 465–473.
[3] I.A.H. van den Berk, M. Kanglie, T.S.R. van Engelen, S. Bipat, M.G.W. Dijkgraaf, P. M.M. Bossuyt, W. de Monye, J.M. Prins, J. Stoker, OPTimal IMAging strategy in patients suspected of non-traumatic pulmonary disease at the emergency department: chest X-ray or ultra-low-dose CT (OPTIMACT)-a randomised controlled trial chest X-ray or ultra-low-dose CT at the ED: design and rationale, Diagn. Progn. Res. 2 (2018) 20.
[4] K.M. Hintenlang, J.L. Williams, D.E. Hintenlang, A survey of radiation dose associated with pediatric plain-film chest X-ray examinations, Pediatr. Radiol. 32 (11) (2002) 771–777.
[5] R. Ward, W.D. Carroll, P. Cunningham, S.A. Ho, M. Jones, W. Lenney, D. Thompson, F.J. Gilchrist, Radiation dose from common radiological investigations and cumulative exposure in children with cystic fibrosis: an observational study from a single UK centre, BMJ Open 7 (8) (2017), e017548.
[6] A.E. Oestreich, RSNA centennial article: ALARA 1912: "as low a dose as possible" a century ago, Radiographics 34 (5) (2014) 1457–1460.
[7] M.J. Goske, K.E. Applegate, J. Boylan, P.F. Butler, M.J. Callahan, B.D. Coley, S. Farley, D.P. Frush, M. Hernanz-Schulman, D. Jaramillo, N.D. Johnson, S. C. Kaste, G. Morrison, K.J. Strauss, I. Alliance for Radiation Safety in Pediatric, Image Gently(SM): a national education and communication campaign in radiology using the science of social marketing, J. Am. Coll. Radiol. 5 (12) (2008) 1200–1205.
[8] T.L. Slovis, Where we were, what has changed, what needs doing: a decade of progress, Pediatr. Radiol. 41 (Suppl. 2) (2011) 456–460.
[9] M.S. Pearce, J.A. Salotti, M.P. Little, K. McHugh, C. Lee, K.P. Kim, N.L. Howe, C. M. Ronckers, P. Rajaraman, A.W. Sir Craft, L. Parker, A. Berrington de Gonzalez, Radiation exposure from CT scans in childhood and subsequent risk of leukaemia and brain tumours: a retrospective cohort study, Lancet 380 (9840) (2012) 499–505.
[10] J.D. Mathews, A.V. Forsythe, Z. Brady, M.W. Butler, S.K. Goergen, G.B. Byrnes, G. G. Giles, A.B. Wallace, P.R. Anderson, T.A. Guiver, P. McGale, T.M. Cain, J. G. Dowty, A.C. Bickerstaffe, S.C. Darby, Cancer risk in 680,000 people exposed to computed tomography scans in childhood or adolescence: data linkage study of 11 million Australians, BMJ 346 (2013) f2360.
[11] H. Haubenreisser, M. Meyer, S. Sudarski, T. Allmendinger, S.O. Schoenberg, T. Henzler, Unenhanced third-generation dual-source chest CT using a tin filter for spectral shaping at 100kVp, Eur. J. Radiol. 84 (8) (2015) 1608–1613.
[12] T. Tsuda, H. Ishii, S. Ichimiya, M. Kanashiro, J. Watanabe, M. Takefuji, T. Aoyama, S. Suzuki, A. Tanaka, T. Matsubara, T. Murohara, Assessment of in-stent restenosis using high-definition computed tomography with a new gemstone detector, Circ. J. 79 (7) (2015) 1542–1548.
[13] M.J. Siegel, C. Hildebolt, D. Bradley, Effects of automated kilovoltage selection technology on contrast-enhanced pediatric CT and CT angiography, Radiology 268 (2) (2013) 538–547.
[14] H. Yoon, M.J. Kim, C.S. Yoon, J. Choi, H.J. Shin, H.G. Kim, M.J. Lee, Radiation dose and image quality in pediatric chest CT: effects of iterative reconstruction in normal weight and overweight children, Pediatr. Radiol. 45 (3) (2015) 337–344.
[15] B. Karmazyn, Y. Liang, H. Ai, G.J. Eckert, M.D. Cohen, M.R. Wanner, S.G. Jennings, Optimization of hybrid iterative reconstruction level in pediatric body CT, AJR Am. J. Roentgenol. 202 (2) (2014) 426–431.
[16] E. Sorantin, M. Riccabona, G. Stucklschweiger, H. Guss, R. Fotter, Experience with volumetric (320 rows) pediatric CT, Eur. J. Radiol. 82 (7) (2013) 1091–1097.
[17] J. Greffier, A. Hamard, F. Pereira, C. Barrau, H. Pasquier, J.P. Beregi, J. Frandon, Image quality and dose reduction opportunity of deep learning image reconstruction algorithm for CT: a phantom study, Eur. Radiol. 30 (7) (2020) 3951–3959.
[18] J.M. Boone, K.J. Strauss, D.D. Cody, C.H. McCollough, M.F. McNitt-Gray, T.L. Toth, M.J. Goske, D.P. Frush, AAPM Report No. 204: Size-Specific Dose Estimates (SSDE) in Pediatric and Adult Body CT Examinations, American Association of Physicists in Medicine, College Park, Maryland, USA, 2011, p. 30.
[19] C. McCollough, D.M. Bakalyar, M. Bostani, S. Brady, K. Boedeker, J.M. Boone, H. H. Chen-Mayer, O.I. Christianson, S. Leng, B. Li, M.F. McNitt-Gray, R.A. Nilsen, M. P. Supanich, J. Wang, Use of water equivalent diameter for calculating patient size and size-specific dose estimates (SSDE) in CT: the report of AAPM Task Group 220, AAPM Rep. 2014 (2014) 6–23.
[20] A.M. Padole, P. Sagar, S.J. Westra, R. Lim, K. Nimkin, M.K. Kalra, M.S. Gee, M. M. Rehani, Development and validation of image quality scoring criteria (IQSC) for pediatric CT: a preliminary study, Insights Imaging 10 (1) (2019) 95.
[21] A. Romanyukha, L. Folio, S. Lamart, S.L. Simon, C. Lee, Body size-specific effective dose conversion coefficients for CT scans, Radiat. Prot. Dosimetry 172 (4) (2016) 428–437.
[22] T.K. Koo, M.Y. Li, A guideline of selecting and reporting intraclass correlation coefficients for reliability research, J. Chiropr. Med. 15 (2) (2016) 155–163.
[23] AAPM, Pediatric Routine Chest CT Protocol, American Association of Physicists in Medicine, Alexandria, VA, 2017, p. 17.
[24] Y. Takei, O. Miyazaki, K. Matsubara, Y. Shimada, Y. Muramatsu, K. Akahane, K. Fujii, S. Suzuki, K. Koshida, Nationwide survey of radiation exposure during pediatric computed tomography examinations and proposal of age-based diagnostic reference levels for Japan, Pediatr. Radiol. 46 (2) (2016) 280–285.
[25] K.J. Strauss, M.J. Goske, A.J. Towbin, D. Sengupta, M.J. Callahan, K. Darge, D. J. Podberesky, D.P. Frush, C. Maxfield, S.J. Westra, J.S. Prince, H. Wu, M. Bhargavan-Chatfield, Pediatric chest CT diagnostic reference ranges: development and application, Radiology 284 (1) (2017) 219–227.
[26] H. Jarvinen, R. Seuri, M. Kortesniemi, A. Lajunen, E. Hallinen, P. Savikurki-Heikkila, P. Laarne, M. Perhomaa, E. Tyrvainen, Indication-based national diagnostic reference levels for paediatric CT: a new approach with proposed values, Radiat. Prot. Dosimetry 165 (1–4) (2015) 86–90.
[27] R. Zeng, M.A. Gavrielides, N. Petrick, B. Sahiner, Q. Li, K.J. Myers, Estimating local noise power spectrum from a few FBP-reconstructed CT scans, Med. Phys. 43 (1) (2016) 568.
[28] U.J. Schoepf, F.G. Meinel, SpringerLink, Multidetector-Row CT of the Thorax, Springer International Publishing: Imprint: Springer, Cham, 2016.
[29] J.C. O'Daniel, D.M. Stevens, D.D. Cody, Reducing radiation exposure from survey CT scans, AJR Am. J. Roentgenol. 185 (2) (2005) 509–515.
[30] B. Schmidt, N. Saltybaeva, D. Kolditz, W.A. Kalender, Assessment of patient dose from CT localizer radiographs, Med. Phys. 40 (8) (2013), 084301.
[31] P. Nowik, G. Poludniowski, A. Svensson, R. Bujila, F. Morsbach, T.B. Brismar, The synthetic localizer radiograph - a new CT scan planning method, Phys. Med. 61 (2019) 58–63.